Assessment of olive pomace wastes as flame retardants

Elyssa El Kassis, Belkacem Otazaghine, Roland El Hage, Rodolphe Sonnier

Assessment of olive pomace wastes as flame retardants

Elyssa El Kassis,[1,2] Belkacem Otazaghine,[2] Roland El Hage,[1] Rodolphe Sonnier[2]

[1]LCPM, Faculty of Sciences, Lebanese University, Fanar, Lebanon

[2]C2MA, IMT Mines Alés, 6, Avenue de Clavières, 30100 Alès, France

Correspondence to: R. El Hage (E-mail: roland_hag@ul.edu.lb) and R. Sonnier (E-mail: rodolphe.sonnier@mines-ales.fr)

ABSTRACT: Olive pomace (OP) is a lignocellulosic waste from olive oil industry. In order to valorize these wastes as flame retardant (FR) fillers into polymers, OP residues are milled and screened into three different fractions. Two strategies are then investigated. The first one is to modify OP particles by phosphorus molecules using radiation grafting as already done successfully with flax. Nevertheless, pyrolysis combustion flow calorimetry analyses show that the introduction of phosphorus does not promote charring of OP and flame retardancy is not significantly improved whichever the considered fraction. The second strategy is to replace pentaerythritol by OP as char source into well-known FR systems based on ammonium polyphosphate. The incorporation of such system into ethylene-vinyl acetate copolymer leads to satisfying FR performances according to cone calorimeter tests. Moreover, the presence of high amount of extractives into OP such as oleic acid does not appear detrimental.

KEYWORDS: biobased resource; composite; flame retardancy; olive pomace; radiation grafting

INTRODUCTION

Due to environmental concerns, biobased materials are more and more considered as alternatives to oil-based ones. If this strategy to reduce our dependence on nonrenewable resources has first led to the development of biobased polymers as poly(lactic acid), for example, nowadays active researches attempt to develop biobased reinforcements and additives for composite industry. Natural fibers are used in biocomposites in replacement of glass fibers. Various biobased additives can be prepared from biobased resources. This is especially the case for flame retardants (FRs).[1,2]

There are several ways to develop biobased FRs. Of course, most of the researches focus on phosphorus-containing FRs because phosphorus is one key element in flame retardancy and it is considered as benign in comparison to halogens. A first strategy is to modify biobased building blocks with phosphorus groups of interest, as phosphate, phosphonate, or phosphinate.[3] These modified building blocks can be used as additive or reactive groups. Several examples can be found elsewhere.[4,5] A second strategy is to extract biobased compounds able to act themselves as FRs due to their high phosphorus content. For instance, phytic acid can be modified as various metallic phytates.[6] Deoxyribonucleic acid has also been used as intumescent FR.[7]

Some biobased resources can also be used as FR even if it does not contain phosphorus. Lignin has been studied as potential FR due to its high ability to char.[8,9] Basak and Ali have used pomegranate rind extract, a waste rich in nitrogen and polyphenolic components, to improve the flame retardancy of jute.[10] However, in most cases, such biobased resource cannot act as FR itself but can lead to highly efficient FR systems in the presence of phosphorus compounds, as ammonium polyphosphate (APP). This way allows developing FR systems containing a biobased resource as it is, that is, without chemical modification which has a non-negligible environmental cost. For example, intumescent FR systems were developed combining APP and lignin or starch in replacement of common oil-based pentaerythritol (PER).[11] Biobased wastes are especially such desirable resources because their use as FR does not compete with other applications.

Olive pomace (OP) is lignocellulosic waste from olive oil industry. The management of the wastes from olive oil industry is a major environmental issue concerning several countries in Mediterranean area. Only for Lebanon, the olive solid wastes are estimated to 79,000 t per year.[12] OP composition varies according to the source of OP as well as to the preparation processes (grinding) and characterization methods (extraction). Detailed composition is given by Dermeche *et al.*[13] OP contains high amount of lignin and relatively low amount of holocellulose. It also contains a high amount of extractives, mainly oleic acid.

Different ways of OP valorization have been proposed. A comprehensive review about these strategies can be found elsewhere.[13]

Akay *et al.* have attempted to recover olive oil from OP using supercritical CO_2.[14] Recovering high-valuable molecules as phenolic compounds from OP is also intensively investigated.[15–18] OP has been considered as energy source.[19–21] OP may be also valorized as fillers. Djefel *et al.* have combined OP with stearic acid to prepare phase change material.[22]

This waste has already been used in polymers as polypropylene,[23,24] poly(3-hydroxybutyrate-*co*-3-hydroxyvalerate),[24] chitosan,[25] plasticized wheat gluten,[26,27] and mechanical, thermal properties as well as matrix-OP compatibility of resulting composites, were investigated. In order to select more suitable fractions, fractionation of OP was also carried out and its influence on composition and properties was studied.[24,28]

Nevertheless, to the best of our knowledge, OP has not been yet used as a part of FR systems. In this work, the role of OP preparation (fractionation and removal of extractives) on their flammability was first studied. Indeed, as discussed above, the composition of OP may be different according to the fractionation. Moreover, the presence of extractives may modify the flammability of OP, especially its thermal stability and heat of combustion. Then, two ways were explored to use OP as FRs. The first one is the radiation grafting of phosphorus compounds on OP. This process has been already successfully developed for other lignocellulosic materials (flax[29–31]) but never for OP. The second one is to combine APP and OP (in replacement of commonly used PER) in EVA composites.

EXPERIMENTAL

Materials

OP deposit that belongs to 2017 harvest season was obtained from "Ghawi-Ghawi" Olive mills located in Darbechtar Village (North Governorate of the republic of Lebanon). These OPs were obtained using a cold-pressing traditional oil extraction pretreatment based on oil separation through filtering after olives crushing using a rotary mill. Ethylene-vinyl acetate (EVA) copolymer (Escorene Ultra Heva UL 00328–27 wt % of vinyl acetate) was provided by ExxonMobil (Irving, Texas, USA). APP (Exolit AP760) was provided by Clariant (Muttenz, Switzerland). PER was provided by Acros Organics (Geel, Begium). Dimethyl vinyl phosphonate (MVP) was provided by abcr (Karlsruhe, Germany).

Preparation of Materials

Grinding. Partially wet OP residues were dried in ambient air at room temperature for 1 week until a relative moisture content of 5–6% was reached. The dried residues were ground using a simple Waring Laboratory blender during about 50 s at maximum speed. After grinding, sorting process using sieve shaker Octagon allows to separate the OP powder into three fractions (Figure 1). Sieves size was 250, 630, and 800 μm. The coarser fraction (around 40 wt % of the residue) is called stone and is not considered in the present study.

Determination of OP Composition. Moisture was measured using an infrared thermobalance after heating about 5 g of OP at 100 °C during 10 min.

Extractives removal was carried out using Soxhlet washings in toluene/ethanol 2:1 solution during 8 h and then in ethanol overnight. Solvents are removed using a rotary evaporator and OP powders are dried at 80 °C overnight.

Lignin content was measured using so-called Klason protocol.[32] This protocol allows solubilizing all components except lignin. OP particles are added in a 72% H_2SO_4 solution at room temperature during 4 h. Then, the mixture is diluted with distilled water and refluxed during 4 h. The mixture is then filtrated and solid residue is dried at 103 °C up to constant mass.

Holocellulose (i.e., cellulose and hemicelluloses) content was measured after dissolving lignin from OP free extractives particles according to ASTM D1104-56.[33] OP particles are added in a flask containing 1 mL of glacial acetic acid, 1 g of $NaClO_2$, and 125 mL of water. The mixture is heated under reflux. A total of 1 g of $NaClO_2$ is added every 2 h up to complete bleaching of particles. The white solid residue corresponding to holocellulose is then dried at 103 °C during 24 h.

Radiation Grafting. As already stated in the Introduction section, irradiation process has already been used to graft phosphorus compounds onto lignocellulosic substrates. The process is called mutual grafting because irradiation and grafting occur in the same time. This procedure involves three steps as already explained in previous works.[29–31] In the first step, 2 g of OP was dipped 1 min into a tetrahydrofuran (THF) solution containing 10 wt % of MVP. After drying to remove solvent, OP was irradiated in air at room temperature using an electron beam accelerator (energy 9.8 MeV) by Ionisos SA (Chaumesnil, France). The applied radiation dose was 50 kGy. In the third step, each irradiated fraction was washed to remove the unbounded monomers, oligomers, or polymers. Washing was carried out for 1 min at room temperature with THF and water successively. Finally, a third washing was carried out using a Soxhlet apparatus with toluene–ethanol (2:1) during 8 h and ethanol during one night.

Preparation of Composites. Composites with various contents of EVA, OP, APP, and PER were first prepared using an internal mixer (HAAKE PolyLab System, R3000) equipped with a 300 cm^3 tank. Temperature, rotor speed, and blending time were fixed, respectively, at 150 °C, 60 rpm, and 10 min.

Squared specimens (100 × 100 × 4 mm^3) were then obtained using a hydraulic forming press (Darragon, 100 T) at 150 °C and 30 bars with a first heating step of 3 min and a compression step of 3 min.

The composites composition is shown in Table I.

Characterizations

A Beckman Coulter LS13320 laser diffraction particle size analyzer instrument was used to determine the size distribution of OP fractions. Size measurements were performed using the microliquid module (15 mL) in THF; obscuration was 10 ± 2%. Optical Fraunhofer model was used.

A scanning electron microscopy (SEM; FEI Quanta 200 ESEM) was used to observe OP and composites. All micrographs were recorded under high vacuum.

The Py-gas chromatography/mass spectrometry (GC/MS) analytical setup consisted of an oven pyrolyzer connected to a GC/MS

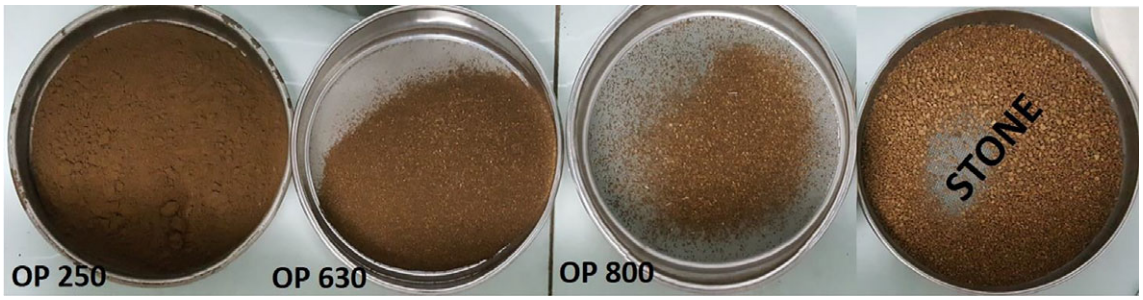

Figure 1. OP fractions after grinding and sieving. [Color figure can be viewed at wileyonlinelibrary.com]

system. A Pyroprobe 5000 pyrolyzer (CDS Analytical) was used to pyrolyze the samples in a helium environment. This pyrolyzer is supplied with an electrically heating platinum filament. One coil probe enables the pyrolysis of samples (<1 mg) placed in quartz tube between two pieces of quartz wool. The sample is flash pyrolyzed at 900 °C or alternatively successively heated at 300, 500, 700, and 900 °C. Each temperature was held for 15 s before gases were drawn to the GC for 5 min. The pyrolysis interface was coupled to a 450-GC (Varian) by means of a transfer line heated at 270 °C. In this oven, the initial temperature of 70 °C was held for 0.2 min, and then raised to 310 °C at 10 °C min^{-1}. The column is a Varian Vf-5 ms capillary column (30 m × 0.25 mm) and helium (1 mL min^{-1}) was used as the carrier gas; a split ratio was set to 1:50. The gases were introduced from the GC transfer line to the ion trap analyzer of the 240-MS (Varian) through the direct-coupled capillary column. Identification of the products was achieved comparing the observed mass spectra to those of the National Institute of Standards and Technology mass spectral library.

Phosphorus content was measured after acid mineralization by inductively coupled plasma atomic emission spectroscopy (ICP–AES; ACTIVA-M, Horiba, Japan). The calibration was performed using commercial nitric acid standard solutions which had the following phosphorus concentrations: 0, 5, 25, and 100 mg L^{-1}. A spectral range of 213–618 nm was used.

Thermogravimetric analyses (TGAs) were performed using a SETSYS Evolution apparatus (Setaram, Caluire, France). Then, 10 (±2) mg of samples were heated under nitrogen flow (100 mL min^{-1}) at a heating rate equal to 1 °C s^{-1} from ambient to 900 °C after a first isotherm at 30 °C lasting 30 min.

Fuel production was investigated using a pyrolysis combustion flow calorimeter (PCFC from Fire Testing Technology, East Grinstead, UK) which was developed by Lyon and Walters.[34] The sample (3 ± 0.5 mg) was heated from 80 to 750 °C at 1 °C s^{-1} in a pyrolyzer under nitrogen flow and the degradation products were sent to a combustor where they are mixed with oxygen in excess at 900 °C. In such conditions, these products were fully oxidized. Heat release rate (HRR) was then calculated by oxygen depletion according to Huggett's relation[35] (1 kg of consumed oxygen corresponds to 13.1 MJ of released energy).

Fire behavior was also studied using a cone calorimeter (Fire Testing Technology). A horizontal sample sheet of 100 × 100 × 4 mm^3 was placed at 25 mm below a conical heater and insulated by rock wool. The samples were exposed at a heat flux of 35 kW m^{-2} in well-ventilated conditions (air rate 24 L s^{-1}) in the presence of a spark igniter to force the ignition. HRR was determined according to oxygen depletion (Huggett's relation) as in PCFC. This test was performed according to the ISO 5660 standard.

RESULTS

Preparation and Characterization of OP Wastes

OP was ground and three fractions were separated from the coarsest part called stone (this fraction was not considered in the work).

These fractions exhibit all a unimodal distribution (Figure 2). The modes are 177, 450, and 864 μm, respectively, for OP 250, OP 630, and OP 800. Particles have a low aspect ratio and angular shape as evidenced by SEM pictures (Figure 3). All particles of the smallest fraction have a size lower than 500 μm.

Composition was assessed by selective extraction and dissolution processes. Moisture is about 5 wt % in good agreement with Lammi *et al.*[28] (Table II). Extractives content is constant for the three fractions (27–30 wt %). Lignin content is high in comparison to other lignocellulosic materials. Its content is the lowest for

Table I. Composites Prepared in this Study

Sample	EVA	APP	PER	OP 250-E	OP 250
90EVA/10OP-E[a]	90	0	0	10	0
80EVA/10APP/10OP-E	80	10	0	10	0
70EVA/20APP/10OP-E	70	20	0	10	0
70EVA/20APP/10OP[b]	70	20	0	0	10
70EVA/20APP/10PER	70	20	10	0	0
60EVA/30APP/10OP-E	60	30	0	10	0

[a] E corresponds to OP with extractives.
[b] Extractives free.

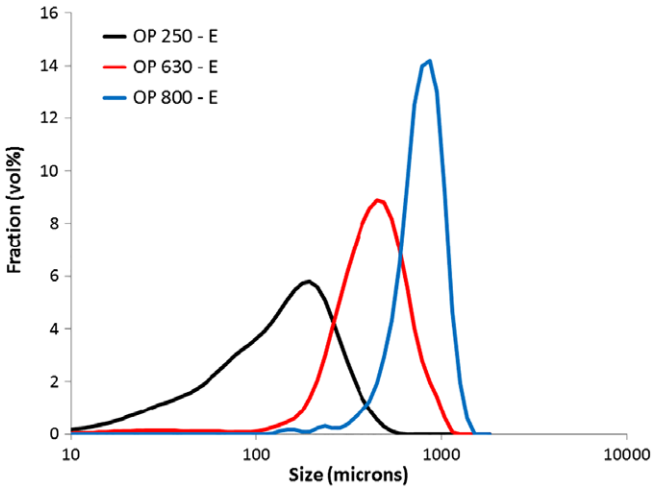

Figure 2. Size distribution of OP fractions. [Color figure can be viewed at wileyonlinelibrary.com]

the smallest particles (27 wt % of mass after extractives removal) but increases to 55–64 wt % for the coarsest fractions. Holocellulose (i.e., hemicelluloses and cellulose) was assessed for OP 250 and OP 630. Its content is similar (56–58 wt % of mass after extractives removal). Note that the sum of lignin and holocellulose contents is slightly lower than 100% for OP 250 and higher than 100% for OP 630 because measurements were achieved from a separate analysis and because soluble lignin present in the aqueous phase was not measured after filtration. In addition, extractions of lignin and holocellulose are not fully selective processes. Therefore, some lignocellulosic components and residual extractives might be extracted into both fractions.

It is quite difficult to compare these values with data proposed in the literature because the different analyzed components as well as the methods of extractives are not always the same.

Py-GC/MS analyses were carried out on the smallest fraction of OP (OP 250), especially to identify the nature of extractives. In the first analysis, the sample was heated at 900 °C (Figure 4). It can be observed the presence of an intense peak at 22 min, corresponding to oleic acid. Oleic acid is the main fatty acid present in

Table II. Composition of OP Fractions

	OP 250-E	OP 630-E	OP 800-E
Moisture (wt %)	6	5	5
Extractives (wt % of dry mass)	32	31	29
Lignin (wt % of mass after extractives removal)	27	55	64
Holocellulose (wt % of mass after extractives removal)	56	58	NA

OP, far ahead palmitic acid and linoleic acid.[36,37] This peak is very intense in OP containing extractives (OP-E) and other peaks are almost unobservable. Oleic acid is also found in OP fraction after washing to remove extractives, evidencing that this removal is not complete. Nevertheless, the peak is less intense. Other peaks can be assigned to aromatic rings and especially phenols and may correspond to lignin decomposition.

Analyses were also carried out at various temperatures to better identify the different decomposition steps and corresponding released products (Figure 5). It is noteworthy that oleic acid is found in the whole range of decomposition temperature for OP-E, even if the corresponding peak is especially intense at 300 and 500 °C. On the contrary, oleic acid is found only at 300 °C for OP after extractives removal treatment. Due to its long aliphatic chain, oleic acid as main component of extractives may have a significant influence on OP flammability.

HRR and thermogravimetry curves are shown in Figures 6 and 7. (Main flammability data of extractives and OP are shown in Table S1.) Extractives decomposition occurs in several steps, the main one is located at 280 °C. Total heat release (THR) and heat of complete combustion are high (respectively, 30 and 34 kJ g^{-1}). Such values are close to the heat of combustion of oleic acid (37.9 kJ g^{-1}) which is the main component of extractives. OP-E fractions are similar and exhibit two low apparent peaks (90–100 W g^{-1}). The first one is around 250 °C and the second one is close to

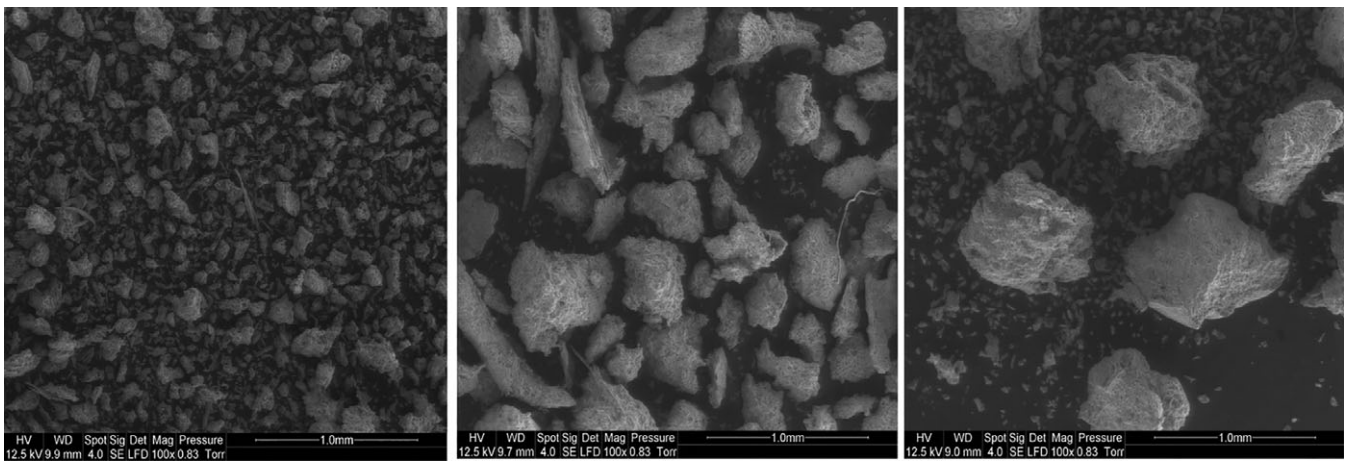

Figure 3. SEM pictures of OP fractions (left OP 250, middle OP630, and right OP 800).

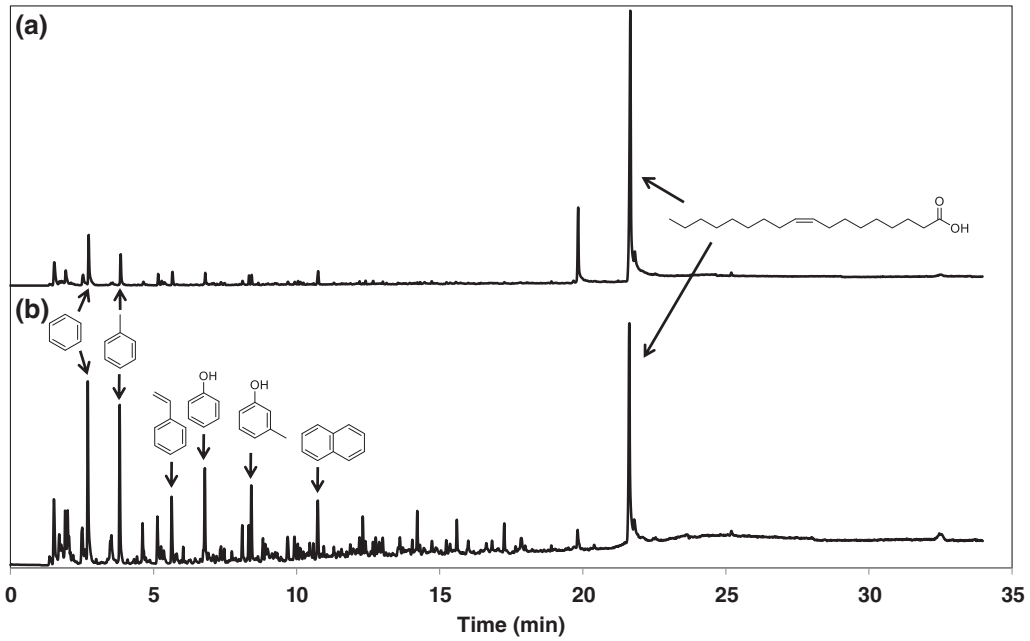

Figure 4. Py-GC/MS analyses for (a) OP 250-E and (b) OP 250 (flash pyrolysis at 900 °C).

350 °C. THR is quite high in comparison to other lignocellulosic materials as natural fibers,[38] in the range 12.6–14.9 kJ g^{-1}. Char content is close to 20 wt % and heat of combustion is therefore in the range 16–18 kJ g^{-1}. Barbanera *et al.*[19] and Miranda *et al.*[20] have found values around 20–22 kJ g^{-1} for OP pellets while Guizani *et al.* found a lower value of 17.2 kJ g^{-1}.[21] All these values were measured using oxygen bomb calorimeter, that is, for aerobic pyrolysis. Therefore, the values are significantly higher than THR measured in the present study.

After extractives removal, the first peak at 250 °C fully disappears. Nevertheless, the HRR curves above 300 °C remains unchanged in comparison to OP-E samples with a peak at 350–360 °C and a shoulder at 300 °C. THR decreases from 12.6–14.9 to 9.2–10.3 kJ g^{-1}. Note that the removal of 30 wt % of extractives with THR of 30 kJ g^{-1} corresponds roughly to this difference. Char is also slightly enhanced for OP samples after extractives removal, except for the coarser fraction. Once again, there are few (negligible) differences between the three OP fractions.

TGAs were carried out for several samples (Figure 6). OP samples without extractives exhibit similar curves. A first peak at low temperature (100 °C) is ascribed to moisture release (around 5 wt %). Two peaks of mass loss rate (pMLR) are observed at 280 and 350 °C. They should correspond, respectively, to the shoulder and the peak observed in PCFC. Char content is around 25 wt % at

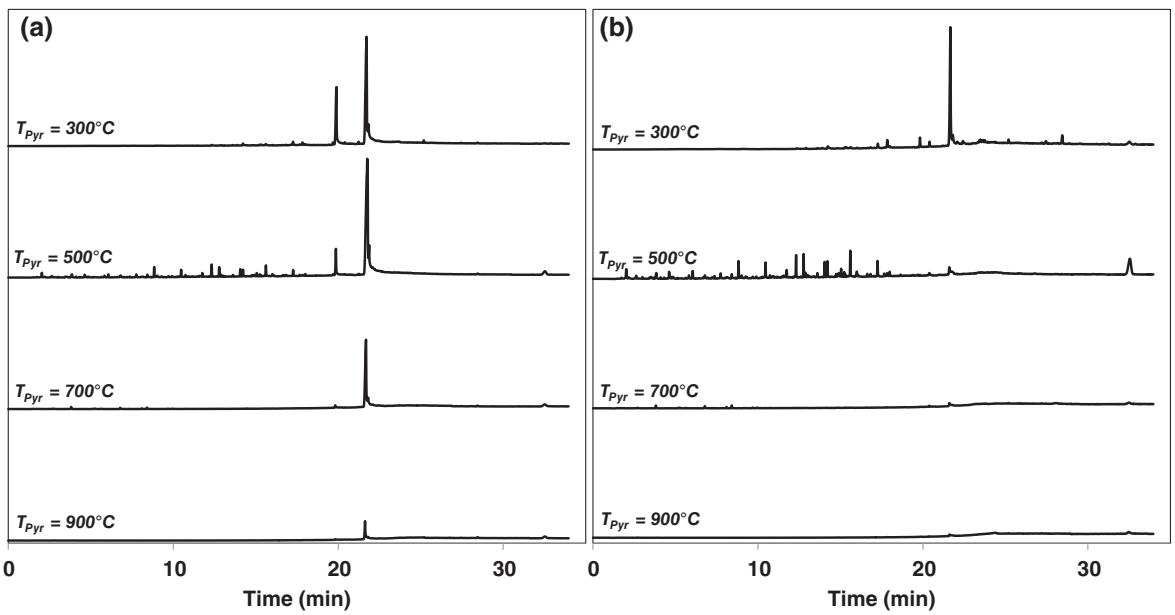

Figure 5. Py-GC/MS analyses for (a) OP 250-E and (b) OP 250 (successive flash pyrolysis at 300, 500, 700, and 900 °C).

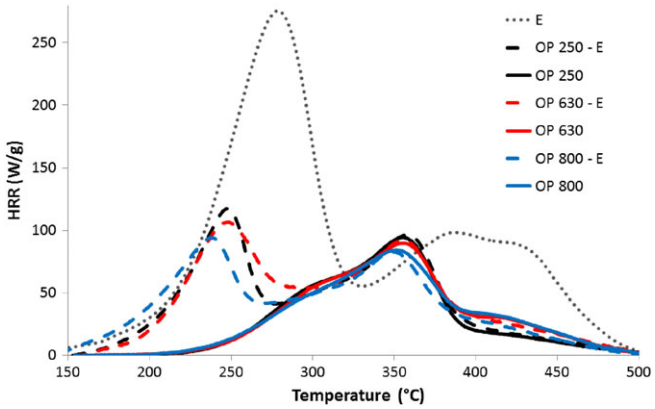

Figure 6. HRR curves versus temperature for OP fractions from PCFC analyses. [Color figure can be viewed at wileyonlinelibrary.com]

750 °C. OP 250-E sample exhibits a much higher pMLR at 280 °C probably due to the presence of extractives. While three decomposition steps are observed in PCFC (two peaks at 280 and 360 °C and one shoulder at 300 °C), only two peaks are observed in TGA. It can be assumed that the first peak merges the two first steps observed in PCFC. Char content is also reduced for OP 250-E (15 wt %) in good agreement with the findings in PCFC.

First Strategy: Radiation Grafting of Phosphorus on OP

Phosphorus compounds have already successfully grafted onto lignocellulosic materials as flax[29–31] using irradiation. The content of phosphorus depends on a couple of parameters and the flammability was directly dependent on this content. Briefly, the THR, peak of HRR, temperature at peak of heat release rate (pHRR) and heat of combustion decrease while char content increases when phosphorus content increases. While OP is also lignocellulosic material, the same strategy was carried out using MVP. This FR was already used to be radiation grafted on flax.[29]

Phosphorus content was assessed after dipping, irradiation, and different washing steps for the three OP fractions. Phosphorus contents after dipping and after irradiation were calculated from weighting and considering that extractives were removed during dipping. Indeed, this assumption appears quite reasonable. PCFC analyses show that the first pHRR assigned to extractives disappears for modified OPs. Nevertheless, if a small content of extractives is not removed during dipping, phosphorus contents should be slightly lower than those calculated in Table III.

Phosphorus content after dipping is high for the three OP fractions. It decreases after irradiation due to partial MVP volatilization between dipping and irradiation. This phenomenon was already identified in previous works. After washing, the phosphorus content decreases drastically. Despite a high MVP impregnation, phosphorus content is lower than 1 wt % in all cases. This value was the minimum to improve significantly the flame retardancy of flax. THF washing is not the most efficient one to remove all the ungrafted phosphorus monomers and macromolecules. Water and Soxhlet washings allow to extract further molecules and phosphorus content becomes very low (<0.5 wt %).

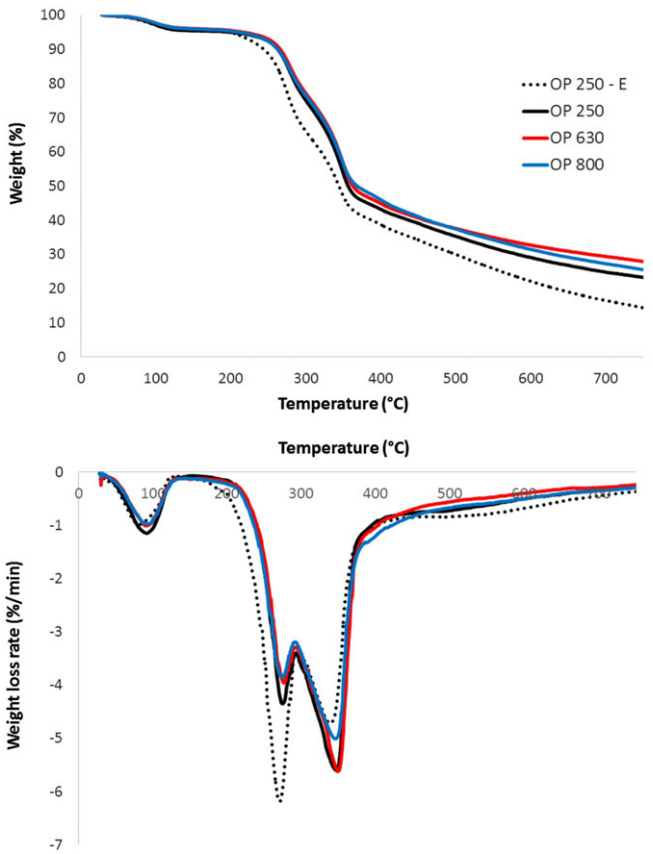

Figure 7. (a) TGA and (b) differential thermogravimetry curves for OP fractions. [Color figure can be viewed at wileyonlinelibrary.com]

Flammability of modified OP samples was investigated using PCFC (Table IV). Figure 8 shows the change in HRR curves for OP 250 after the different modification steps. The influence of phosphorus is the same for the three fractions. A decrease in THR is observed from around 14 kJ g^{-1} for OP containing extractives to 8 kJ g^{-1} for OP after dipping and drying. This decrease corresponds mainly to the disappearance of the first pHRR initially at

Table III. Phosphorus Contents after each Processing Steps for the Three OP Fractions

Wt % phosphorus	After dipping[a]	After irradiation[a]	After THF washing[b]	After THF and water washing[b]	After THF, water, and Soxhlet washing[b]
OP 250-E	4.6	3.7	0.88	0.32	0.24
OP 630-E	6.4	4.6	0.94	0.32	0.2
OP 800-E	5.5	NA	0.46	0.22	0.12

[a] From weighting.
[b] From ICP-AES measurements.

Table IV. Phosphorus Contents after each Processing Steps for the Three OP Fractions

	THR (kJ g^{-1})	Main pHRR (W g^{-1})	Temperature at main pHRR (°C)	Residue (%)	Other pHRR (W g^{-1})	Temperature of other pHRR (°C)
OP 250						
OP 250-E	14.3	96	358	20	112	249
OP 250	9.2	95	356	25	X	X
+Dipping into 10% MVP solution	8.1	76	357	27	44	297
+Irradiation at 50 kGy	7.5	71	323	19	14	212
+THF washing	8.1	80	316	20	X	X
+Water washing	10.7	87	335	20	X	X
+Soxhlet washing	10.2	92	341	20	X	X
OP 630						
OP 630-E	14.9	87	354	17	90	256
OP 630	10.1	92	356	22	X	X
+Dipping into 10% MVP solution	7.9	71	351	27	29	254
+Irradiation at 50 kGy	6.3	66	314	19	X	X
+THF washing	8.1	80	316	20	X	X
+Water washing	9.4	80	329	23	X	X
+Soxhlet washing	10.1	86	337	20	X	X
OP 800						
OP 800-E	12.6	86	356	21	74	232
OP 800	10.3	88	353	20	X	X
+Dipping into 10% MVP solution	7.4	76	366	23	46	303
+Irradiation at 50 kGy	7.5	71	327	18	X	X
+THF washing	9.3	79	338	13	60	295
+Water washing	9.5	87	339	22	X	X
+Soxhlet washing	9.9	93	353	20	X	X

250 °C (called other peak in Table IV). The second peak (called main peak in Table IV) is only slightly decreased from 90–100 to 70–75 W g^{-1}. This peak is still observed at 350–360 °C. Residue increases from 17–20 to 27 wt %. In fact, the OP fractions after dipping and drying exhibit HRR curves very close to those of the counterpart fractions without extractives. THR and pHRR are only slightly lower. It can be assumed that the main effect of the dipping into THF solution is the removal of extractives and phosphorus has quite low influence on flammability.

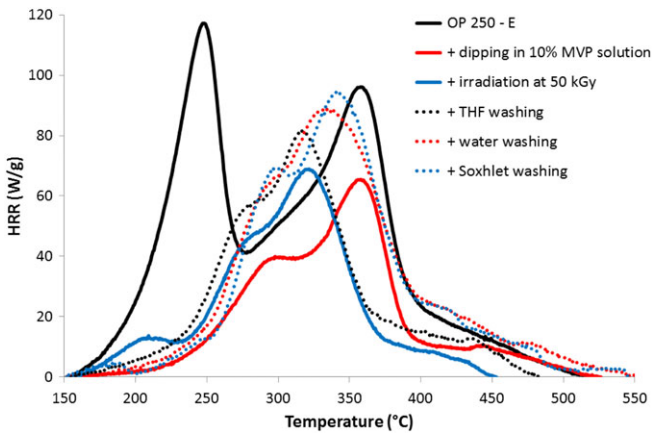

Figure 8. HRR curves versus temperature for OP 250-E after the different modification steps from PCFC analyses. [Color figure can be viewed at wileyonlinelibrary.com]

After irradiation, a slight decrease in THR and pHRR is observed despite lower phosphorus content. Nevertheless, the main impact of irradiation is a decrease in char content and thermal stability. Char content decreases to 19–20 wt % while the temperature of the pHRR decreases significantly from 350–360 to 310–320 °C. These changes cannot be assigned to the phosphorus presence but to irradiation (or to the combination of phosphorus and irradiation). This is quite surprising. When such process was carried out with flax, the thermal stability decreased due to the phosphorus FR even before irradiation. Moreover, irradiation alone provokes only a negligible decrease of flax thermal stability. Similarly, char from flax depends only on phosphorus content whether or not there is irradiation.

After washing, the phosphorus content decreases drastically. THR and pHRR increase slightly while char content is stable around 20 wt % (the low value for OP 800 after THF washing is due to experimental uncertainties). Temperature of pHRR is also enhanced up to 340 °C. The whole curves are very close to those of OP without extractives, but the thermal stability is reduced.

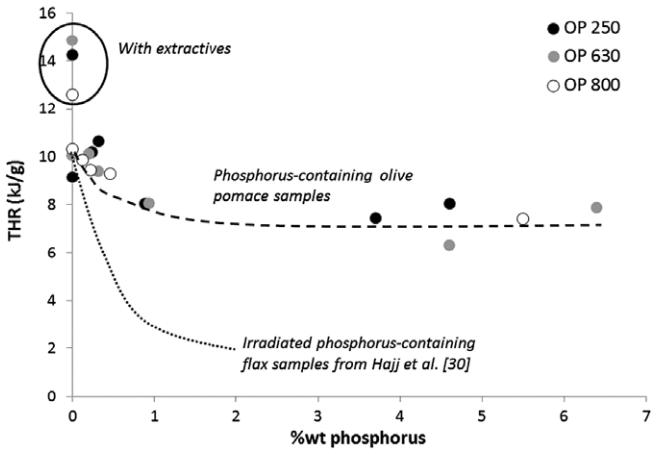

Figure 9. THR versus phosphorus content for modified OP fractions from PCFC analyses.

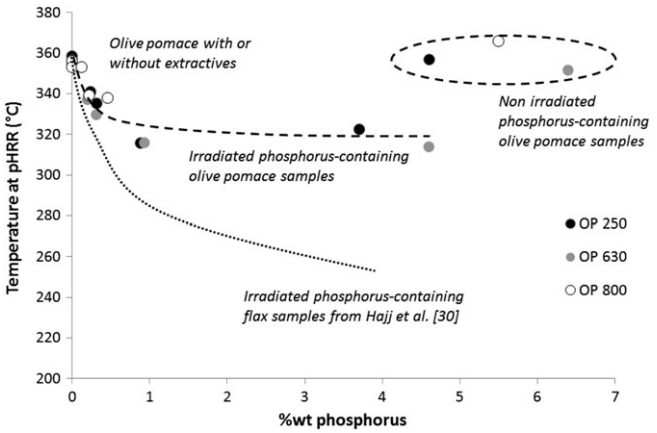

Figure 11. Temperature at pHRR versus phosphorus content for modified OP fractions from PCFC analyses.

Figures 9–11 summarize the main data from Table IV and compare them to similar data obtained in our previous works for flax fabrics modified using radiation grafting.[30] They point out the two main findings discussed just above. First, the phosphorus FR has a limited influence of OP flammability in comparison to flax. Char is little enhanced and THR decreases only slightly. Second, irradiation of phosphorus-containing OP leads to a strong decrease in thermal stability and char content. In the case of flax, the thermal stability as well as the char promotion are only dependent on phosphorus content and not on radiation dose (in the dose range considered).

Finally, the radiation grafting of phosphorus compounds cannot be considered as a suitable strategy to prepare FR OP: the phosphorus content is too limited after washing steps and it does not significantly reduce the flammability of OP.

Second Strategy: APP-OP Combination

The second strategy is to use OP as char source to promote the formation of an insulating char layer in the presence of a char promoter as APP. Typically, APP can be used alone in polymers able to char as polyesters or polyamides. However, in EVA or polyolefins, it must be combined with char source as PER. PER is oil-based and OP may be a biobased alternative to PER.

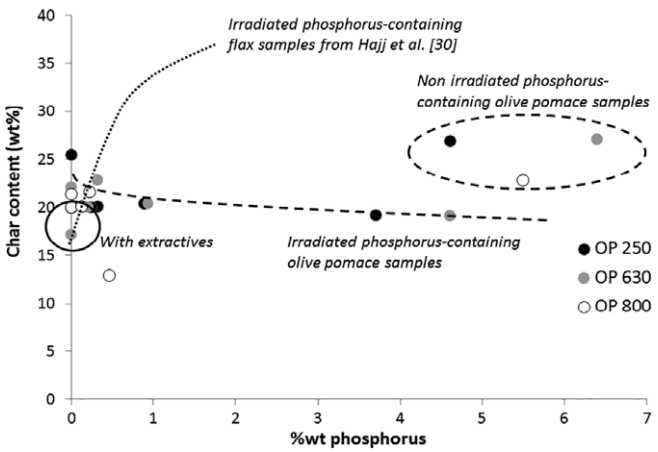

Figure 10. Char content versus phosphorus content for modified OP fractions from PCFC analyses.

The smallest fraction of OP was incorporated at a content of 10 wt % with various amounts of APP. It is well known that the best ratio between APP and char source is between 2:1 and 3:1. PER was incorporated with APP at a ratio of 2:1 for comparison. Moreover, a formulation with 20 wt % of APP and 10 wt % of OP without extractives was also prepared to assess the influence of extractives. Indeed, extractives represent around 30 wt % of OP, their heat of combustion is high, and their thermal stability is quite low. Therefore, they may make ignition earlier.

Dispersion of additives (APP, PER, and OP) was assessed using SEM–energy-dispersive X-ray spectroscopy (EDX; Figure 12). Pictures are shown for two formulations. OP particles and APP can be easily observed: OP particles size ranges from several dozens to hundreds of micrometers. APP particles are smaller and appear brighter due to the presence of phosphorus. Particles are well dispersed in EVA matrix. PER has a high melting point and therefore it does not melt during processing. Therefore, it can be found as very large particles (>200 μm) in 70EVA/20APP/10PER. APP particles are well dispersed in the matrix.

Flammability of EVA composites was first assessed using PCFC (Figure 13 and Table S2). This device allows comparing samples in well-controlled conditions. Nevertheless, keep in mind that some FR modes-of-action are not effective in this test. This is especially the case of intumescent phenomenon because very small samples are thermally thin and char cannot act as insulating protective barrier.

HRR curves are similar for all composites. Two pHRRs are observed. The first one at 350 °C can be assigned to acetic acid released from EVA decomposition. The second one at 480 °C is due to the decomposition of polyenes formed by acetic acid release. Heat released from OP is much lower than heat released from EVA. Nevertheless, considering HRR curves of OP (see Figure 6), this heat is mainly released around 350 °C and then this decomposition step is overlapped with the first one from EVA. This is probably the reason why this pHRR is constant even when EVA content decreases: this decrease is compensated by a higher content in OP. The decomposition of extractives at lower temperature is not observed because its

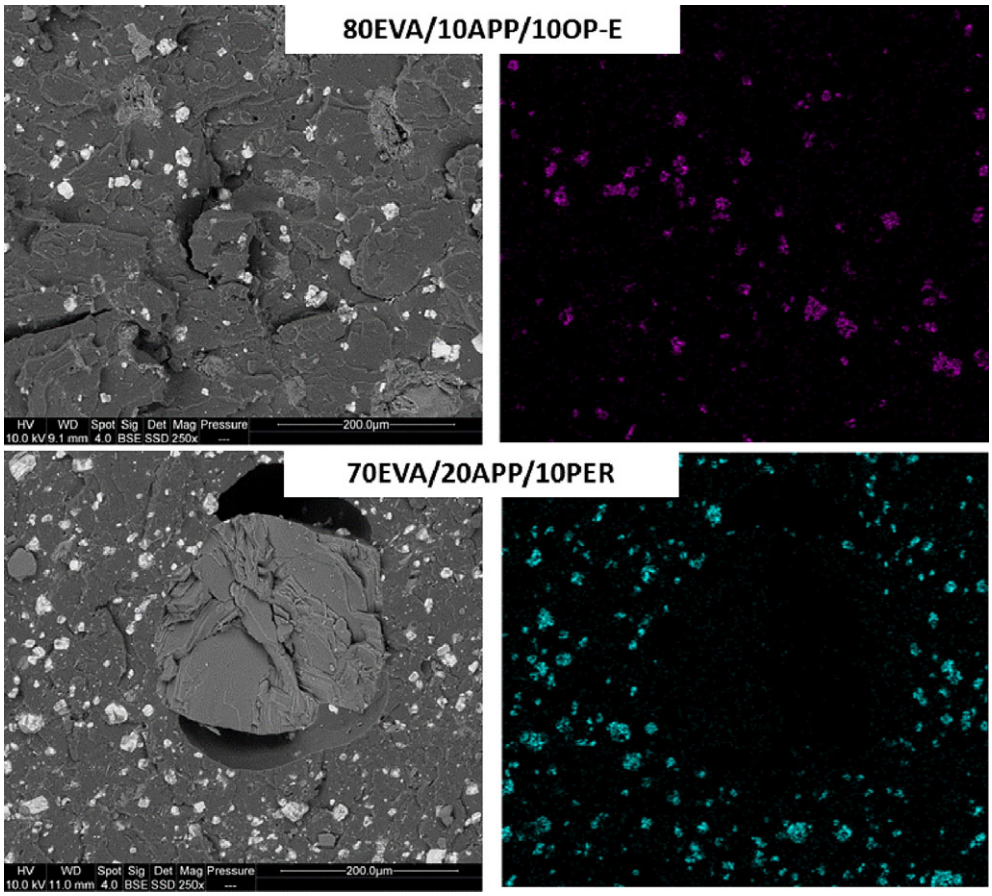

Figure 12. SEM pictures and phosphorus mapping from EDX for some EVA composites. [Color figure can be viewed at wileyonlinelibrary.com]

intensity is too weak. Therefore, there is no difference between 70EVA/20APP/10OP and 70EVA/20APP/10OP-E samples.

The main differences between the composites can be ascribed to the EVA content. When EVA content decreases, THR and main pHRR decrease. Moreover, char content increases because OP (or PER) is able to char, especially in the presence of APP (EVA is not able to char significantly even with APP). Heat of complete combustion also decreases. Indeed, heat of combustion for EVA (around 35 kJ g^{-1}) is much higher than for OP.

APP allows OP to char efficiently. Char content for 80EVA/10APP/10OP-E is 10 wt % versus only 1 wt % for 90EVA/10OP-E. When APP content increases, the char content also increases up to 19 wt % for 60EVA/30APP/10OP-E. It is expected that this char could produce a cohesive layer able to limit heat and gases transfer between flame and material during burning, as cone calorimeter test. Finally, it can be observed that flame retardancy is unchanged when PER is replaced by OP. Flammability data are highly similar for 70EVA/20APP/10OP, 70EVA/20APP/10OP-E, and 70EVA/20APP/10PER.

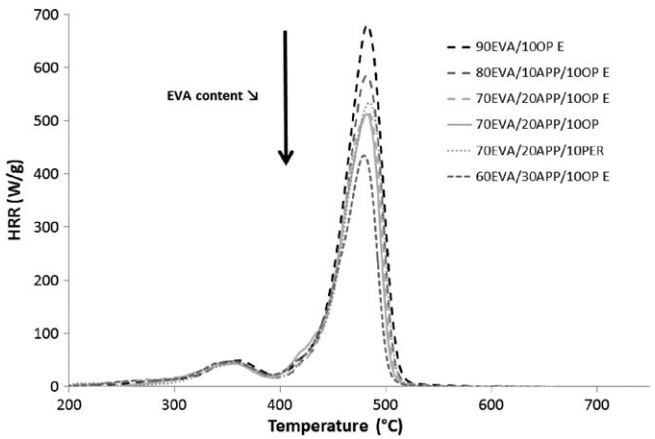

Figure 13. HRR curves versus temperature for EVA composites from PCFC analyses.

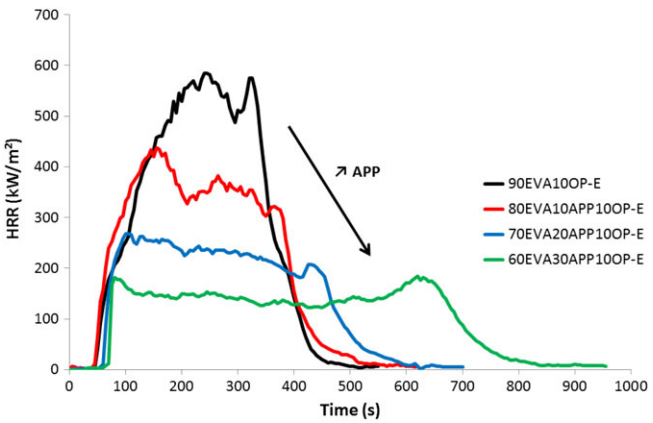

Figure 14. HRR curves versus time for EVA composites containing OP-E from cone calorimeter tests. [Color figure can be viewed at wileyonlinelibrary.com]

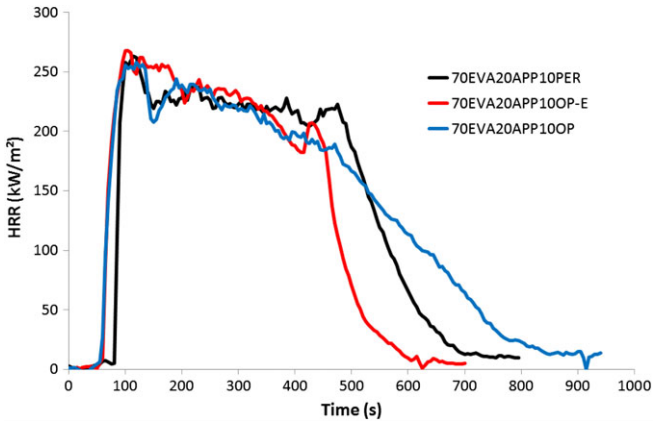

Figure 15. HRR curves versus time for EVA composites containing 20 wt % of APP from cone calorimeter tests. [Color figure can be viewed at wileyonlinelibrary.com]

Cone calorimeter tests are needed to give a correct insight of flammability at bench scale. Curves and main data can be found in Figures 14 and 15 and Table S3. 90EVA/10OP-E burns easily with a quite low time-to-ignition, a high pHRR (613 kW m^{-2}) and almost no residue. The addition of APP allows to improve significantly the flame retardancy of EVA composites. Time-to-ignition increases, especially for 30 wt % of APP. Peak of HRR decreases and char content increases continuously as shown in Figure 16. THR also decreases due to the decrease in EVA matrix which represents the most flammable component. The effective heat of combustion also decreases slightly. Note that the curve shape of 90EVA/10OP-E corresponds to an intermediate thick noncharring behavior. It turns into thick charring behavior when 10 and 20 wt % of APP are incorporated. HRR is controlled and the curve exhibits a quasi-plateau. The plateau is clearly observed at a low HRR value with 30 wt % of APP. Moreover, in that case, an additional peak can be found at the end of the test. This peak may be due to the breaking of the char layer or to the accumulation of heat leading to an increase of pyrolysis rate at the bottom of the sample.

Pictures (Figure 17) confirm that char is formed for composites containing APP, but it is not intumescent. Note that the char surface is more cohesive for 60EVA/30APP/10OP-E. It may be

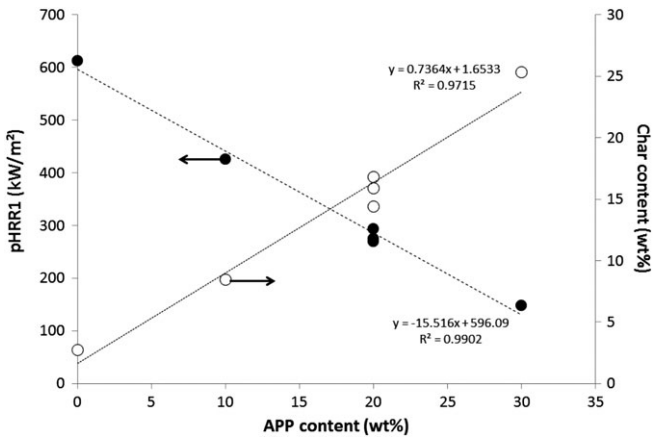

Figure 16. pHRR1 and char content versus phosphorus content for EVA composites from cone calorimeter tests.

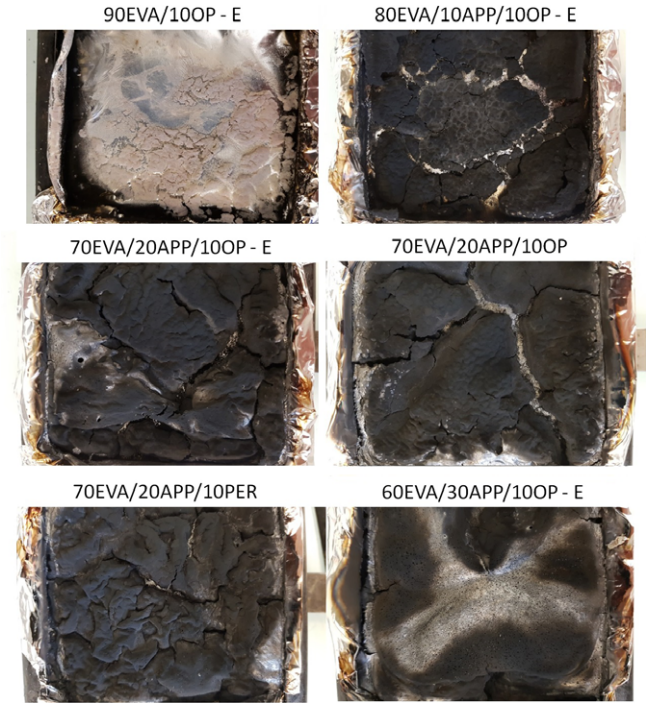

Figure 17. Pictures of residues obtained after cone calorimeter tests. [Color figure can be viewed at wileyonlinelibrary.com]

concluded that the char layer is more efficient for this formulation and it is confirmed by the high residue content (25 vs. 19 wt % at microscale). This discrepancy between char contents in cone calorimeter and PCFC tests may be indicative that the char prevents the full pyrolysis of the composite. For the other formulations, residue content is similar in cone calorimeter and PCFC tests.

Combustion efficiency, calculated as the ratio between the effective heat of combustion and the heat of complete combustion (measured in PCFC) ranges between 0.87 and 1. It means that the combustion is almost complete and no flame inhibition is observed, as it is usual for FR systems based on APP.

The comparison of the three composites containing 20 wt % of APP is shown in Figure 15. It is obvious that there is no significant difference in terms of pHRR (270–300 kW m^{-2}), THR (23–25 kJ g^{-1}), heat of combustion (28–30 kJ g^{-1}), or char content (around 15 wt %). Only Time-to-ignition (TTI) is higher for 70EVA/20APP/10PER (78 s vs. 54–55 s). The removal of extractives does not lead to higher TTI or lower flammability. Therefore, it can be considered that OP can replace PER as biobased char source and no extractives removal is needed.

CONCLUSIONS

OP is a lignocellulosic waste containing a large amount of extractives (mainly oleic acid) but also lignin. Therefore, its use as char source in the presence of phosphorus to improve the flame retardancy of polymers needs to be assessed.

OP contains a large amount of lignin and a high ability to char. Extractives content is also high (around 30 wt %) and increases

significantly the flammability of OP due to high heat of combustion of oleic acid. THR is close to 14 kJ g^{-1} in the presence of extractives and only 9–10 kJ g^{-1} after extraction.

The radiation grafting of phosphorus FRs leads to disappointing results in comparison to previous findings obtained with flax or miscanthus substrates. Indeed, phosphorus does not lead to a significant decrease in THR or to an increase in char content. Moreover, irradiation seems to be very detrimental for thermal stability of OP. It can be also noted that there is no difference between the different OP fractions despite various compositions, especially in terms of lignin content.

The combination of APP and OP into EVA composites leads to very satisfying results and HRR curve is similar to that found with well-known combination of APP and PER. Moreover, the presence of extractives has no significant impact on flammability, at least for moderate amount of OP (10 wt %, corresponding to around 3 wt % of extractives). OP can be considered as valuable biobased char source alternative to PER.

ACKNOWLEDGMENTS

The authors acknowledge the Ecole des Mines d'Alès for supporting the FERIA project (Prix André Lefebvre). This project has been jointly funded with the support of the National Council for Scientific Research in Lebanon CNRS-L and Lebanese University (NOMISOL-2018/2020). Romain Ravel, Benjamin Gallard, and Loïc Dumazert are acknowledged for their help in the preparation and characterization of materials. The authors acknowledge Sophie Rouif and Ionisos Company for irradiation of samples. Acknowledgments are also addressed to Jamil Ghawi who provided us the olive pomace and the various information related to the pretreatment process that these residues have undergone.

REFERENCES

1. Sonnier, R.; Taguet, A.; Ferry, L.; Lopez-Cuesta, J. M. Towards Bio-Based Flame Retardant Polymers; Springer: Cham, Switzerland, **2018**.
2. Costes, L.; Laoutid, F.; Brohez, S.; Dubois, P. *Mater. Sci. Eng.: R: Rep.* **2017**, *117*, 1.
3. Illy, N.; Fache, M.; Ménard, R.; Negrell, C.; Caillol, S.; David, G. *Polym. Chem.* **2015**, *6*, 6257.
4. Ménard, R.; Negrell, C.; Ferry, L.; Sonnier, R.; David, G. *Polym. Degrad. Stab.* **2015**, *120*, 300.
5. Negrell, C.; Frénéhard, O.; Sonnier, R.; Dumazert, L.; Briffaud, T.; Flat, J. J. *Polym. Degrad. Stab.* **2016**, *134*, 10.
6. Costes, L.; Laoutid, F.; Dumazert, L.; Lopez-Cuesta, J. M.; Brohez, S.; Delvosalle, C.; Dubois, P. H. *Polym. Degrad. Stab.* **2015**, *119*, 217.
7. Alongi, J.; Carletto, R.; Di Blasio, A.; Carosio, F.; Bosco, F.; Malucelli, G. *J. Mater. Chem. A*. **2013**, *1*, 4779.
8. Gallina, G.; Bravin, E.; Badalucco, C.; Audisio, G.; Armanini, M.; De Chirico, A.; Provasoli, F. *Fire Mater.* **1998**, *22*, 15.
9. Song, P.; Cao, Z.; Fu, S.; Fang, Z.; Wu, Q.; Ye, J. *Thermochim. Acta*. **2011**, *518*, 59.
10. Basak, S.; Ali, S. W. *Polym. Degrad. Stab.* **2017**, *144*, 83.
11. Reti, C.; Casetta, M.; Duquesne, S.; Bourbigot, S.; Delobel, R. *Polym. Adv. Technol.* **2008**, *19*, 628.
12. Kinab, E.; Khoury, G. *Renew. Sustain. Energy Rev.* **2015**, *52*, 209.
13. Dermeche, S.; Nadour, M.; Larroche, C.; Moulti-Mati, F.; Michaud, P. *Process Biochem.* **2013**, *48*, 1532.
14. Akay, F.; Kazan, A.; Soner Celiktas, M.; Yesil-Celiktas, O. *Supercrit. Fluids*. **2015**, *99*, 1.
15. Leouifoudi, I.; Harnafi, H.; Zyad, A. *Adv. Pharmacol. Sci.* **2015**, 1.
16. Aliakbarian, B.; Paini, M.; Adami, R.; Perego, P.; Reverchon, E. *Innov. Food Sci. Emerg. Technol.* **2017**, *40*, 2.
17. Chanioti, S.; Tzia, C. *Innov. Food Sci. Emerg. Technol.* **2018**, *48*, 228.
18. Pagnanelli, F.; Cruz Viggi, C.; Toro, L. *Appl. Surf. Sci.* **2010**, *256*, 5492.
19. Barbanera, M.; Lascaro, E.; Stanzione, V.; Esposito, A.; Altieri, R.; Bufacchi, M. *Renew. Energy*. **2016**, *88*, 185.
20. Miranda, T.; Arranz, J.; Montero, I.; Roman, S.; Rojas, C.; Nogales, S. *Fuel Process. Technol.* **2002**, *103*, 91.
21. Guizani, C.; Haddad, K.; Jeguirim, M.; Colin, B.; Limousy, L. *Energy*. **2016**, *107*, 453.
22. Djefel, D.; Makhlouf, S.; Khedache, S.; Lefebvre, G.; Royon, L. *Internat. J. Hydrogen Energy*. **2015**, *40*, 13764.
23. Kaya, N.; Atagur, M.; Akyuz, O.; Seki, Y.; Sarikanat, M.; Sutcu, M.; Seydibeyoglu, M. O.; Sever, K. *Compos. Part B*. **2018**, *150*, 277.
24. Lammi, S.; Le Moigne, N.; Djenane, D.; Gontard, N.; Angellier-Coussy, H. *Ind. Crop Prod.* **2018**, *120*, 250.
25. de Moraes Crizel, T.; de Oliveira Rios, A.; Alves, V.; Bandarra, N.; Moldao-Martins, M.; Hickmann Flores, S. *Food Hydrocoll.* **2018**, *74*, 139.
26. Boudria, A.; Hammoui, Y.; Adjeroud, N.; Djerrada, N.; Madani, K. *Adv. Powder Technol.* **2018**, *29*, 1230.
27. Hammoui, Y.; Molina-Boisseau, S.; Duval, A.; Djerrada, N.; Adjeroud, N.; Remini, H.; Dahmoune, F.; Madani, K. *Mater. Des.* **2015**, *87*, 742.
28. Lammi, S.; Barakat, A.; Mayer-Laigle, C.; Djenane, D.; Gontard, N.; Angellier-Coussy, H. *Powder Technol.* **2018**, *326*, 44.
29. Sonnier, R.; Otazaghine, B.; Viretto, A.; Apolinario, G.; Ienny, P. *Eur. Polym. J.* **2015**, *68*, 313.
30. Teixeira, M.; Sonnier, R.; Otazaghine, B.; Ferry, L.; Aubert, M.; Tirri, T.; Wilén, C. E.; Rouif, S. *Radiat. Phys. Chem.* **2017**, *145*, 135.
31. Hajj, R.; El Hage, R.; Sonnier, R.; Otazaghine, B.; Gallard, B.; Rouif, S.; Nakhl, M.; Lopez-Cuesta, J. M. *Polym. Degrad. Stab.* **2018**, *147*, 25.
32. Brosse, N.; El Hage, R.; Chaouch, M.; Pétrissans, M.; Dumarçay, S.; Gérardin, P. *Polym. Degrad. Stab.* **2010**, *95*, 1721.

33. ASTM D1104-56 Method of Test for Holocellulose in Wood; ASTM International: West Conshohocken, USA, **1978**.
34. Lyon, R. E.; Walters, R. N. *Anal. Appl. Pyrol.* **2004**, *71* (1), 27.
35. Huggett, C. *Fire Mater.* **1980**, *4*(2), 61.
36. Wedyan, M.; Abu Hanieh, B.; Al Harasheh, A.; Rahman Al Tawaha, A. *Bulg. J. Agric. Sci.* **2017**, *23*, 866.
37. Clemente, A.; Sanchez-Vioque, R.; Vioque, J.; Bautista, J.; Millan, F. *Food Biotechnol.* **1997**, *11*, 273.
38. Dorez, G.; Ferry, L.; Sonnier, R.; Taguet, A.; Lopez-Cuesta, J. M. *Anal. Appl. Pyrol.* **2014**, *107*, 323.